

(will be inserted by hand later)

Your thesaurus codes are:

ASTRONOMY
AND
ASTROPHYSICS
28.6.1995

NASA-CR-200895

Rotational periods and starspot activity of young solar-type dwarfs in the open cluster IC 4665 ^{*}

S. Allain¹, J. Bouvier¹, C. Prosser², L.A. Marschall³, and B.D. Laaksonen³¹ Laboratoire d'Astrophysique, Observatoire de Grenoble, URA CNRS 708, Université Joseph Fourier, B.P. 53, 38041 Grenoble Cedex 9, France, allain/bouvier@gag.observ-gr.fr² Harvard-Smithsonian Center for Astrophysics, 60 Garden Street, MS-66, Cambridge, MA 02138, prosser@cfa.harvard.edu³ Gettysburg College, Dept. of Physics, Gettysburg, PA 17325, marschal/s207723@gettysburg.edu

Received date; accepted date

Abstract. We present the results of a V-band photometric monitoring survey of 15 late-type dwarfs in the young open cluster IC 4665. Low-amplitude periodic light variations are found for 8 stars and ascribed to the modulation by starspots that cover typically a few percent of the stellar disk. Periods range from 0.6 to 3.7d, translating to equatorial velocities between 13 and 93 km.s⁻¹. That no period longer than 4d was detected suggests a relative paucity of extremely slow rotators ($V_{eq} < 10$ km.s⁻¹) among late-type dwarfs in IC4665. The fractional number of slow rotators in IC 4665 is similar to that of Alpha Per cluster, suggesting that IC 4665 is close in age to Alpha Per (~ 50 Myr).

Key words: Stars: activity (08.01.2); Stars: late-type (08.12.1); Stars: rotation (08.18.1); Open clusters: individual: IC 4665 (10.15.2 IC 4665)

1. Introduction

Young open clusters with ages of a few 10 Myr harbour a large number of solar-type stars that are just starting their evolution onto the main sequence. Their peculiar evolutionary status, right at the transition between pre-main sequence and main-sequence evolution, make these stars particularly interesting laboratories for testing current models and ideas on the evolution of magnetic activity, angular momentum and lithium abundance from the earliest phases of evolution up to the age of the Sun.

It was the unexpected discovery by Van Leeuwen & Alphenaar (1982, see also Van Leeuwen et al. 1987) of a few extremely rapidly rotating late-type dwarfs in the Pleiades, with rotational velocities in excess of 100 km.s⁻¹, that prompted

Send offprint requests to: J. Bouvier

^{*} Based on observations made at the Observatoire de Haute-Provence (CNRS), France, Mt. Hopkins Whipple Observatory, CTIO, and the National Undergraduate Research Observatory, U.S.A.

the subsequent thorough studies of rotation in young clusters. These studies, which so far mostly focused on two young clusters, Alpha Persei (50 Myr) and the Pleiades (70 Myr), led to the determination of the distribution of rotational velocities for large samples of late-type dwarfs on the ZAMS (see the review by Stauffer 1991). Contemporaneously, statistical studies of the rotational properties of low-mass pre-main sequence T Tauri stars led to the determination of the distribution of rotation among stars with an age of only a few Myr (see the review by Bouvier 1991). Thus at the beginning of the 90's, the distributions of projected velocities, $\delta(v \sin i)$, of both low-mass PMS and ZAMS stars were sufficiently well known to be used as, respectively, initial and final boundary conditions for modeling the evolution of angular momentum of solar-type stars during the pre-main sequence (and beyond when combined with $v \sin i$ measurements of late-type dwarfs in older clusters and of the field).

The main challenge for these models is to account for the fact that while T Tauri stars have a relatively narrow $\delta(v \sin i)$ peaking around 20 km.s⁻¹, young cluster stars exhibit a much wider $\delta(v \sin i)$ extending from a few km.s⁻¹ up to almost 200 km.s⁻¹. Recent studies suggest that the rotational evolution of T Tauri stars is largely dictated by the interaction between the star and its circumstellar disk (Bouvier et al. 1993, Edwards et al. 1993). More specifically, the lower rotation rates measured for T Tauri stars interacting with their disk compared to those of T Tauri stars lacking a disk suggests that accretion of circumstellar material results in the braking of the central star. Several models have recently been proposed to describe this braking effect that occurs in spite of accretion of circumstellar material of high specific angular momentum onto the star. They all rely on the assumption that the star/disk interaction is mediated by a strong stellar magnetic field (Königl 1991, Shu et al. 1994, King & Regev 1994).

This disk-braking process might help to understand the co-existence of slow and rapid rotators on the ZAMS, as observed among late-type dwarfs in young clusters: stars which dissipate

their disk at the beginning of their PMS evolution freely spin up as they contract to the ZAMS while stars that retain their disk for a longer time are strongly braked and reach the ZAMS as slow rotators (Hartmann 1991, Bouvier 1994). While quite an appealing explanation for the observed widening of $\delta(v\sin i)$ between the T Tauri phase and the ZAMS, the braking effect by the disk depends upon several parameters which are unfortunately not well determined, namely: the strength of the stellar magnetic field and its topology, the mass-accretion rate and its temporal evolution, and the lifetime of circumstellar disks.

A constraint currently lacking to test the validity of this scenario is the determination of the *true* rotation rates of the slowest rotators in young clusters. So far, rotational studies of late-type dwarfs in young clusters were mostly restricted to the measurement of projected velocities, $v\sin i$. As a result, only *upper limits* of 7 to 10 km.s^{-1} are currently set on the equatorial velocities of the slowest ZAMS rotators. While an equatorial velocity of $\simeq 7 \text{ km.s}^{-1}$ on the ZAMS can conceivably result from the disk-braking process assuming reasonable values for the star's magnetic field, accretion rate, and disk lifetime (e.g., Cameron & Campbell 1993), a much lower velocity of $\simeq 2\text{-}3 \text{ km.s}^{-1}$ would be much more difficult to account for. The measurement of *equatorial* rotation rates, as opposed to projected velocities, for the slowest rotators in young clusters is therefore of primary importance to assess the required efficiency of the disk-braking process during PMS evolution.

Direct determination of equatorial stellar rotation rates can be obtained through photometric monitoring with the aim of detecting rotational modulation induced by stellar spots: the period of modulation seen in the star's light-curve is then a direct measurement of the star's rotational period free of any geometric effects. In this paper, we report on results from the photometric monitoring study of late-type dwarfs belonging to the young cluster IC 4665 [17h44m, +5°40' (1950)]. IC 4665 is one of the few open clusters easily observable from the northern hemisphere during summer months. The cluster is relatively nearby ($\sim 350\text{pc}$) and has recently been extensively investigated in order to identify solar-type and low-mass cluster members through proper motion, photometry, and radial velocity observations (Prosser 1993, Prosser & Giampapa 1994). IC 4665 is also a relatively young cluster (Prosser & Giampapa 1994), being similar in age to the nearer Pleiades and α Persei clusters. Concurrent with other studies of stellar rotation and activity of solar-type stars among the Pleiades, α Per, and field T Tauri stars, we decided to investigate IC 4665's membership to determine true rotational periods which may be used to compare IC 4665 to other nearby clusters in regards to rotational velocity distributions and activity/rotation relations.

In Section II, we describe how the stellar sample was selected and observed. In Section III, the stellar light-curves are analyzed and rotational periods derived. We discuss the implications of these results for the evolution of angular momentum during the pre-main sequence in Section IV.

2. Sample selection, observations and data reduction

Our initial sample consisted of 27 IC4665 candidate members selected from the list of Prosser (1991;1993). The stars were restricted to the $0.50 < B-V < 1.40$ range (i.e., spectral types F0-K7); subsequent observations [Prosser 1993, Prosser & Giampapa 1994] identified 12 stars as non-members or likely non-members which we discard in the present analysis. The results for the remaining members and candidate members are reported here.

Observations were conducted at Observatoire de Haute-Provence from June 4 to 17, 1993, with the 120cm telescope equipped with a 512² Tektronics CCD (6.5' FOV). A standard Johnson V-band filter was used for all the observations. Flat-fields and biases were obtained nightly for subsequent image reduction using the NOAO/IRAF CCDRED package. Each of the 20 stellar fields was observed from 1 to 4 times per night almost every night.

For some stars, supporting observations were obtained using the Whipple Observatory 1.2m telescope on Mt. Hopkins, AZ by observer CP and using the 0.8m telescope of the National Undergraduate Research Observatory (NURO) in Flagstaff, AZ by observers LM/BL. Observations by CP were obtained during UT June 27-30, 1993 for P27, P100, P107, P146, and P150. Observations by LM/BL were obtained during UT August 14-18, 1993 for P100, P107, P146, and P150. P27 was also monitored by CP at the CTIO 0.9m telescope during UT Apr 4-6, 1993.

The photometric reduction of the CCD images was performed using the NOAO/IRAF packages APPHOT for uncrowded fields, and DAOPHOT for crowded fields (Stetson 1987). In both cases, aperture photometry was conducted with annular sky background subtraction. Differential photometry between the star of interest and typically 2 to 4 comparison stars in the same image was obtained. For each light curve, object and comparison stars, we subtracted the average of the curve, to obtain zero-averaged curves. The light curves of the non-variable comparison stars were summed to get the reference light curve which contains the non-intrinsic sources of variability due to, e.g., changing atmospheric conditions. The reference light curve thus obtained was then subtracted from the raw light curve of the star of interest to derive its intrinsic light curve.

The photometric error was computed from the dispersion between the light curves of the various comparison stars. The error ranges typically from 0.005 to 0.01 mag. Images leading to a dispersion larger than 0.01 mag among the comparison stars were discarded.

Relative V magnitudes between the object and the reference stars are available upon request to the author.

3. Results

We searched for a periodic signal in the light curves using three different methods. The first method uses the periodogram time-series analysis algorithm for unevenly spaced data (Scargle 1982, Horne & Baliunas 1986). Based on discrete Fourier

Table 1. Stellar properties and photometric periods and amplitudes. Nobs gives the total number of measurements. (See text Section 3)

P	V	B-V	Sp.T.	R/R _⊙	Nobs	period day	V _{eq} km.s ⁻¹	v sin i km.s ⁻¹	sin i	amplitude mag	rms mag	notes
4	11.36	0.49	F0	1.4	28			90-100			0.004	=K37
12	12.71	0.76	G0	1.1	24	0.60 ± 0.01	93 ± 10	≤ 10	≤ 0.1	0.03	0.01	
19	11.97	0.60			22			≤ 10			0.007	SB2
21	11.44	0.50	F1-F2	1.4	22			38			0.002	=K53
27	12.65	0.76	G0	1.1	96	1.54 ± 0.01	36 ± 4	33	0.92	0.03	0.01	SB?
38	12.42	0.67	F7	1.1	24		72	67	0.93	0.08	0.015	(1)
39	12.92	0.72	F9	1.0	23	3.7 ± 0.3	14 ± 3	15	1	0.04	0.01	
71	13.65	0.93	G6	1.0	19	3.0 ± 0.2	17 ± 3	17	1	0.04	0.02	
75	13.68	0.88	G5	0.9	19	2.5 ± 0.1	18 ± 2	16	0.89	0.05	0.02	
94	14.26	1.01	G8	0.8	22			10			0.03	
100	14.34	1.02	K0	0.85	91	2.27 ± 0.02	19 ± 2	21	1	0.1	0.03	
107	12.96	0.82	G2-G3	1.1	86			27			0.01	
146	14.18	1.09	K0	1.0	83			≤ 10			0.01	
150	13.08	0.85	G4	1.1	91	2.22 ± 0.02	25 ± 3	25	1	0.06 & 0.09	0.025	
155	13.41	0.88	G5	0.9	20	2.4 ± 0.1	19 ± 3	17	0.89	0.07	0.03	

(1) A period of 18.6h has been derived by Prosser (1993).

transform, the algorithm computes the power spectrum of the data set called periodogram. We derived the confidence level of the periodogram's peaks by randomly generating a large number of synthetic, pure noise light curves having the same temporal sampling as the object's light curve. These synthetic light curves are then analyzed with the periodogram and the frequency with which a peak appears at a given power provides the false-alarm probability. In the following we consider periods to be real only if a confidence level of 99% or more is reached.

In addition, we applied the CLEAN algorithm from Roberts et al. (1986) to the periodogram analysis. The CLEAN algorithm performs a nonlinear deconvolution in the frequency domain, handling effects due to the finite time span of the data set and the incompleteness of the sampling which generates spurious periods called aliases. When several periods are detected at a high confidence level in the periodogram, CLEANing the periodogram helps to distinguish between real periods and aliases.

We also used the string-length method (Dworetzky 1983) which, for a given trial period, computes the mean length between successive points of the phased light curve. This method does not make any hypothesis upon the light curve's shape and is therefore sometimes more appropriate than the periodogram analysis (though most of the time the results obtained by the two methods are similar).

We were thus able to measure the rotational periods for 8 of the 15 studied stars. The uncertainty on the period was derived from the width at half-maximum of the periodogram peak while the amplitude of photometric variability, ΔV , was derived by fitting a sinusoidal curve, using a least-square method, to the phased light curve. Using the spot model described in Bouvier et al. (1993) we derived from the observed amplitude of modulation in the V-band a crude estimate of the area of the spot

responsible for the photometric variations:

$$\Delta m(\lambda) = -2.5 \log[1 - (1 - Q(\lambda))G_{eq}(\lambda)]$$

where G_{eq} is the lower limit to the true surface (relative to the disk surface) coverage by spots and $Q(\lambda)$ is the flux ratio between the spot and the photosphere. Since we performed observations at only one wavelength, we cannot constrain the spot temperature. We therefore assume an essentially dark spot, whose luminosity is negligible compared to the star luminosity, i.e. $Q(\lambda) = 0$, which yields:

$$G_{eq} = 1 - 10^{-\frac{\Delta m}{2.5}}$$

Once the photometric period, assumed to be a measure of the stellar rotational period, is derived, one can compute the stellar equatorial velocity using an independent estimate of the stellar radius. Here, the stellar radius was estimated from the B-V color and the V magnitude (from Prosser 1993), assuming a distance modulus of $m-M = 8.3$, and a reddening of $E(B-V) = 0.18$ (Mermilliod, 1981) as follows: using tables of $(B-V)_0$ versus effective temperature from Allen (1976, p.206), we get T_{eff} (and the star's spectral type, except for P4, whose spectral type is known from spectroscopic observations). From T_{eff} we compute the bolometric correction, using the Allens's relation (1976, p.197):

$$BC = -42.54 + 10 \log T_{eff} + (29000 K / T_{eff})$$

The bolometric magnitude, M_{bol} , can then be derived as well as the radius from Allen's relation (1976, p.193):

$$M_{bol} = 42.36 - 10 \log T_{eff} - 5 \log (R_* / R_{\odot})$$

i.e.,

$$\frac{R_*}{R_{\odot}} = 10^{-\frac{1}{5}(M_{bol} - 42.36 + 10 \log T_{eff})}$$

A 10% uncertainty is assumed on the stellar radius estimate. Equatorial velocities are then given by $v_{eq} = 2\pi \frac{R_*}{P}$, where P is the rotational period, and can be compared with $v \sin i$ measurements from Prosser & Giampapa (1994).

The results of the period analysis and the stellar properties are summarized in Table 1. The last column of Table 1 gives the rms deviation of the data points in the light curve, as an indication of the degree of photometric variability of the object, regardless of whether a period is detected or not. Below we briefly discuss some of the more noteworthy stars in Table 1.

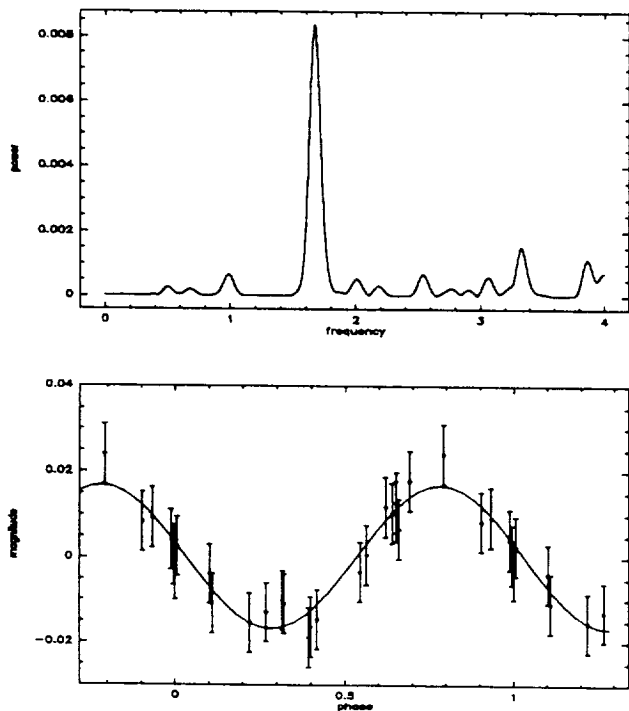


Fig. 1. *Top*: P12 CLEANed periodogram. Frequency (in day^{-1}) is defined as $1/\text{Period}$. *Bottom*: P12's light curve folded in phase with $P=0.6\text{d}$. Magnitude is the difference between V magnitude of the star P12 and the reference stars' magnitude, averaged to zero.

P12: The light curve of P12 shows clear evidence of rapid variations. The raw periodogram gives 3 periods with confidence level of 99.9% : 0.60, 1.47, 3.02, and the string-length method gives as the most probable periods 0.60 and 1.50d. When applying the CLEAN algorithm, only one peak remains at 0.6d (see Fig 1). P12's light curve folded in phase with a period of 0.60d exhibits a smooth sinusoidal-like pattern. We stress, however, that the light-curve sampling (typically 2 measurement per night) is not well suited to detect such short periods. Therefore, this result requires independent confirmation.

The radius is $1.1R_{\odot}$, and assuming a $0.60 \pm 0.01\text{d}$ period, the equatorial velocity is $93 \pm 10\text{km.s}^{-1}$. The $v \sin i$ of P12 is known to be less than 10km.s^{-1} , so it implies that the inclination angle is of the order of 6 degrees, or less. As the

star is seen nearly pole-on, the amplitude of variations (0.03 mag) implies that the spot is located at low latitudes, and has a fractional area of 3% at least.

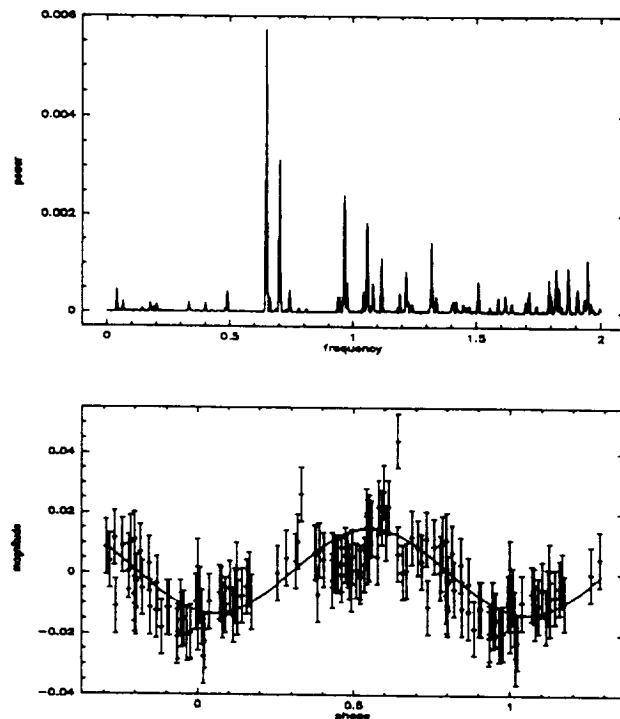


Fig. 2. Same as Fig. 1 for P27 and $P=1.54\text{d}$.

P27: P27 was observed at three epochs: UT April 2 to 6, June 4 to 17 and June 27 to 30, 1993. In the raw periodogram the highest peak corresponds to a period of 1.54d, while the string-length method suggests 1.57 or 2.25d. A period longer than 2d is unlikely as the $v \sin i$ (33km.s^{-1}) corresponds to a maximum period of 1.7d. Analysis with CLEAN indicates a most probable period around 1.57d (see Fig. 2). The light curve over the three epochs of observations and the best sinusoidal fit, obtained with a period of $1.54 \pm 0.01\text{d}$, are shown on Fig. 3. Fig. 2 shows the light curve folded in phase with a period of 1.54d.

The equatorial velocity is $36 \pm 4\text{km.s}^{-1}$, leading to $\sin i = 0.92$. The light curve is well fitted with a sinusoid of amplitude 0.03, which corresponds to a stellar spot of 3% of the stellar disk.

P39: The highest peak in the raw periodogram indicates a period of $3.7 \pm 0.3\text{d}$, with a probability level of $\geq 99.9\%$. An alias is also found at 0.8d with the same probability level. CLEAN confirms that the 3.7d period is the true period (see Fig. 4). The amplitude of variation is 0.04 mag, leading to a spot area of 4% that of the stellar disk. For a radius of $1.0R_{\odot}$ and a $v \sin i$ of 15km.s^{-1} , we find $V_{eq} = 14 \pm 2\text{km.s}^{-1}$ and $\sin i = 1$.

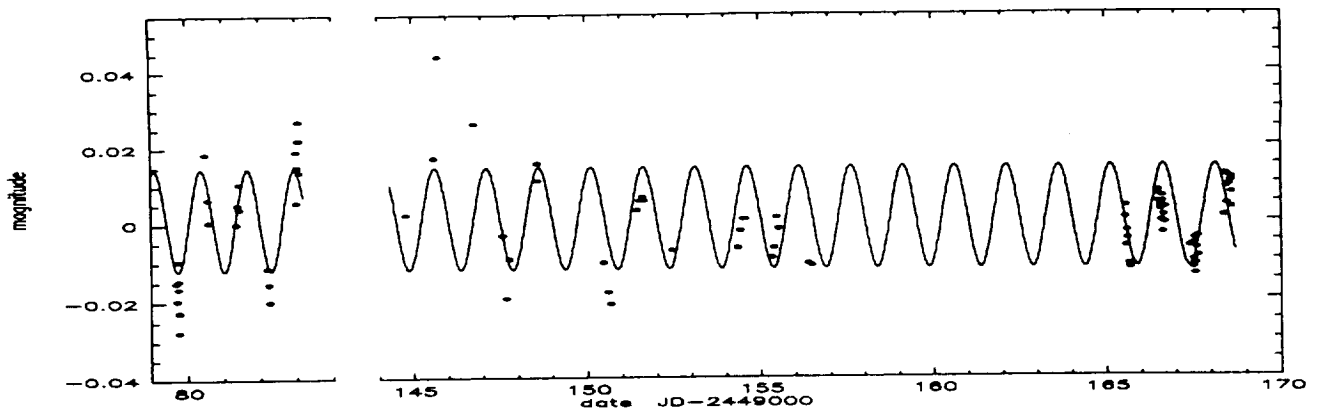


Fig. 3. P27's light curve fitted with a sine curve of period 1.54d.

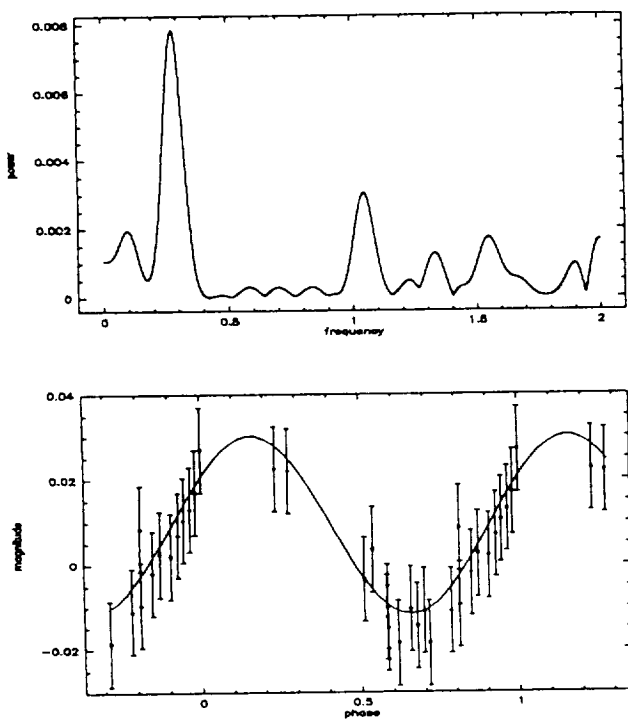


Fig. 4. Same as Fig.1 for P39 and P= 3.7d.

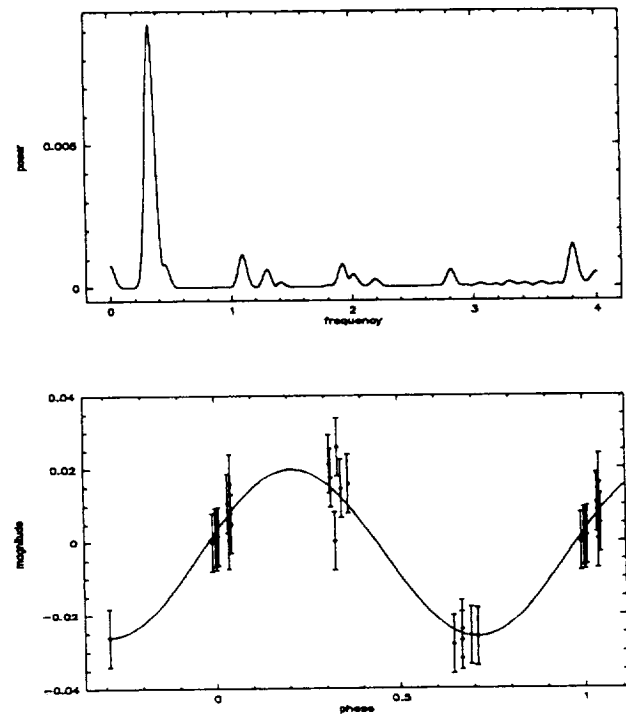


Fig. 5. Same as Fig.1 for P71 and P= 3.0d.

P71: There are two possible periods in the raw periodogram with probability level $\geq 99.9\%$: 3.0 ± 0.2 and 1.50 ± 0.04 d. The CLEANed periodogram only exhibits a peak at a period of 3.0d. Figure 5 shows the light curve fitted with a 3.0d period sinusoid. We deduce a spot coverage of 4% of the stellar disk ($\Delta V = 0.04$) and, for a radius of $1.0R_{\odot}$, $V_{eq} = 17 \pm 3$ km.s⁻¹ consistent with $v \sin i = 17$ km.s⁻¹.

P75: While up to 3 possible periods (0.7, 1.6, and 2.5d) appear at a confidence level $\geq 99.0\%$ in the raw periodogram, only the 2.5 ± 0.1 d period remains after application of the

CLEAN algorithm (see Fig. 6). The amplitude of variation is 0.05 mag, so the spot's fractional area is 4% of the stellar disk. P75's radius is $0.9R_{\odot}$, which gives $V_{eq} = 18 \pm 2$ km.s⁻¹ and $\sin i = 0.89$ for $v \sin i = 16$ km.s⁻¹.

P100: P100 was observed during the following runs: from UT June 4 to 17 at OHP, from UT June 27 to 30 and from UT August 14 to 18, 1993 at NURO. The raw periodogram indicates the following possible periods with high probability levels ($\geq 99.9\%$): 0.68, 1.85 and 2.27d. The string-length method finds a most probable period around 2.26d, and the CLEAN algorithm

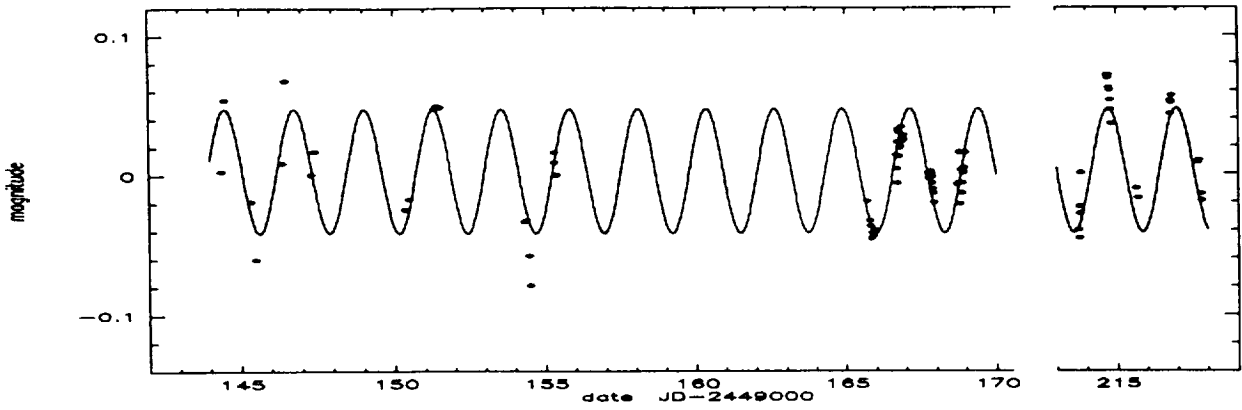


Fig. 8. P100's direct light curve fitted with a sine curve of period $P=2.27$ d.

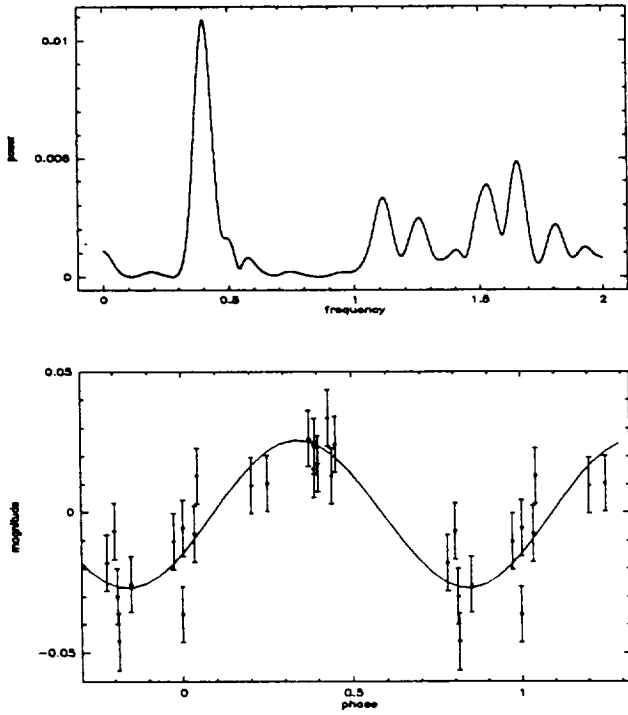


Fig. 6. Same as Fig.1 for P75 and $P=2.5$ d.

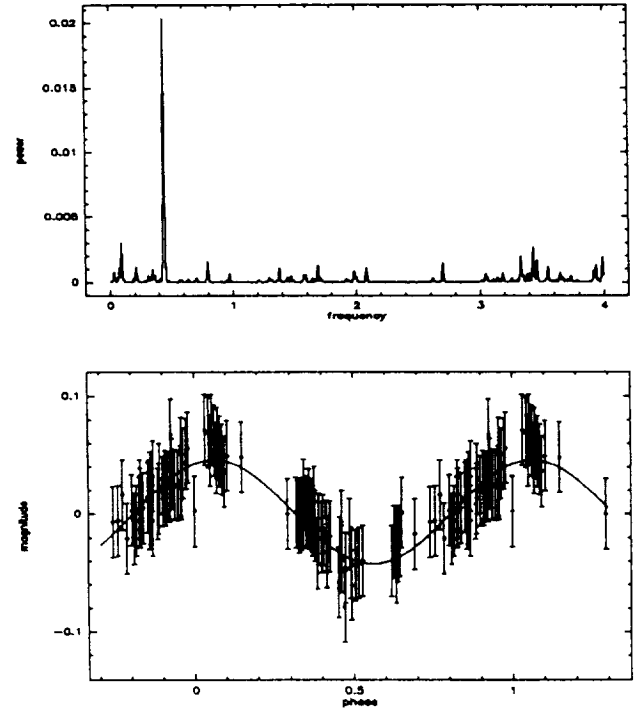


Fig. 7. Same as Fig.1 for P100 and $P=2.27$ d.

confirms with no ambiguity that the 2.27d period is a true period (see Fig. 7). We thus derive a period of $P= 2.27 \pm 0.01$ d for P100. Over the complete observational range (73 days), no phase shift nor variation of the amplitude are observed (Fig. 8).

The amplitude of the variations is 0.1mag (Fig. 7), which corresponds to a dark spot that covers 9% of the stellar disk. For a stellar radius of $0.85 R_{\odot}$, we find $V_{eq} = 19 \pm 2 \text{ km.s}^{-1}$, consistent with $v \sin i = 21 \text{ km.s}^{-1}$ and indicating that the star is seen equator-on.

P150: P150 was observed during three different runs: from UT June 4 to 17 (epoch 1), from UT June 27 to 30 (epoch 2) and from UT August 14 to 18 (epoch 3), 1993. When applied to the entire data set the periodogram and the CLEAN algorithm find with no ambiguity a period of 2.22 ± 0.2 d (Fig. 9 and 10). A sine curve with a period of 2.22d separately fits each of the light curves obtained at the different epochs of observations. It fails, however, to provide a good fit to the whole data set. This suggests that phase shifts and/or amplitude changes occurred within the time span of our observations.

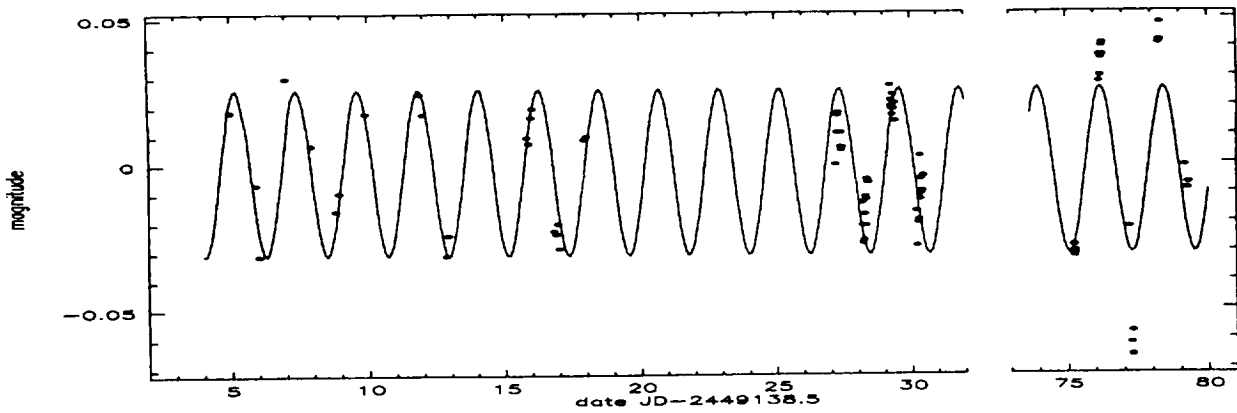


Fig. 10. P150's light curve. A $P=2.22$ d sine curve was fitted to the first epoch of observations (Day 5-18) and extrapolated to the second and third epochs.

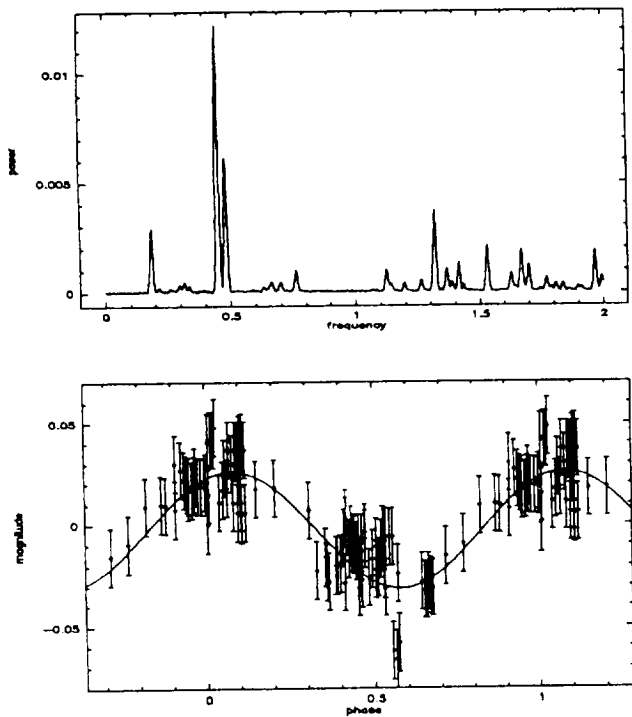


Fig. 9. Same as Fig.1 for P150 and $P=2.22$ d.

That both phase shifts and amplitude changes occurred is apparent on Figure 10. In this figure, the complete light curve is shown together with a sine curve with a period of 2.22d fitted to the first epoch of observations and extrapolated to the second and third ones. It is seen that the amplitude of variations in the second epoch is very similar to that of the first epoch but that the phase has slightly shifted. On the 3rd epoch, it is primarily the photometric amplitude that has changed (0.09 mag compared to 0.06 mag at epoch 1 & 2, which corresponds to a fractional

spot coverage of 8 and 5%, respectively) while the phase is very nearly the same as at epoch 1.

The phase and amplitude changes observed in P150's light curve suggest that the spot properties and/or their location on the stellar surface varies on a timescale shorter than our 2.5 month-long observations. For instance, a longitudinal migration of the spot group at the stellar surface would produce phase shifts qualitatively similar to those observed between epochs 1 & 2. Alternatively, phase shifts may result from the disappearance and reformation of spots at different location on the stellar surface if the spot lifetime is relatively short. That the observed phase shifts from the first to the second and third epochs cannot be accounted for by a *continuously* changing phase, i.e., assuming $\delta\Phi/dt = \text{constant}$, may favor the latter interpretation.

P150 is a G4 spectral type star, for which a $1.1R_{\odot}$ radius and $P=2.22$ d, leads to $V_{eq} = 25 \pm 3 \text{ km.s}^{-1}$. With a measured $v\sin i$ of 25 km.s^{-1} , we thus deduce $\sin i = 1$.

P155: Two possible periods are found again in the periodogram, 1.7d and 2.4d at a confidence level $\geq 99.9\%$. When applying CLEAN only one period remains at $P=2.4 \pm 0.1$ d (Fig. 11). The photometric amplitude of 0.07 mag corresponds to a spot coverage of 6%. For a stellar radius of $0.9R_{\odot}$, we deduce a rotational velocity of $19 \pm 3 \text{ km.s}^{-1}$ and, with a $v\sin i$ of 17 km.s^{-1} , an inclination angle of $i \sim 60^{\circ}$.

P4, P19, P21, P38, P94, P107, P146: No period could be found for these stars. Some do not exhibit photometric variability in excess of the 0.005-0.01 mag photometric error (P4, P19, P21). For the other stars, variability is observed beyond photometric errors but the periodogram did not find any period with a confidence level in excess of 95% (except for P107 where we find marginal evidence for a period between 1.5 and 1.9d). In particular, we are unable to confirm the 18.6h period previously detected for P38 by Prosser (1993) though P38's light curve does suggest rapid photometric variations.

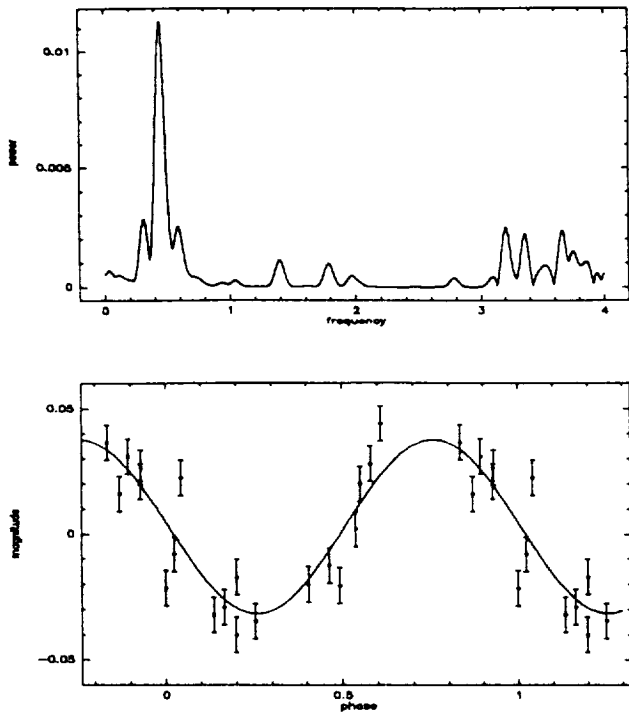


Fig. 11. Same as Fig.1 for P155 and $P=2.4d$.

4. Discussion

Like other young clusters, IC4665 is expected to contain late-type dwarfs near the ZAMS exhibiting a very wide range of rotation rates. In such clusters as Alpha Persei (50 Myr), IC 2391 (30 Myr) and the Pleiades (70 Myr), G and K dwarfs have $v \sin i$ ranging from less than 10 km.s^{-1} to 150 km.s^{-1} or more (Stauffer et al. 1989, Prosser 1992,1994, Soderblom et al. 1993). Although still fragmentary, rotational studies of G-K dwarfs in IC 4665 also indicate a large range of $v \sin i$, from less than 10 km.s^{-1} to at least 70 km.s^{-1} (Prosser & Giampapa 1994).

While $v \sin i$ studies of late-type dwarfs have been quite exhaustive in several young clusters, only a few direct determinations of rotational periods for young cluster dwarfs have been obtained so far. Moreover, recent efforts to derive the rotational periods of young cluster dwarfs have mostly focused on stars with large $v \sin i$ values. The periods of a few hours found for these stars clearly confirm that they are extremely rapid rotators with equatorial velocities up to 200 km.s^{-1} (e.g., Prosser et al. 1993, O'Dell & Collier Cameron 1993).

The measurement of rotational periods for slow rotators is much more demanding. First, long observing runs are needed to sample the light curve over more than one complete rotational cycle. Second, if starspot activity is related to rotation, one might expect the spot size to be smaller in slowly rotating stars than in rapidly rotating ones leading to a corresponding smaller amplitude of photometric modulation. Our primary aim in this

study was to measure rotational periods of slow and moderate rotators in IC 4665. At the time of the observations, the $v \sin i$ of most of the stars in our sample were unknown but were derived since then and are listed in Table 1.

Only 4 stars in the sample (P12, P19, P94, P146) are seemingly slow rotators with a $v \sin i$ of 10 km.s^{-1} or less. We failed to detect a period for 3 of them (P19, P94, P146). One reason might be that these stars are indeed extremely slow rotators, with rotational periods longer than the duration of our observations, i.e., $P \geq 15d$, which would translate into an equatorial velocity of 3 km.s^{-1} at most. Such a small equatorial velocity for a G-K dwarf in a young cluster would imply an extremely efficient braking mechanism acting on stars approaching the ZAMS on their pre-main sequence radiative tracks. Current models of PMS angular momentum evolution of solar-type stars would have severe difficulties to account for such small velocities on the ZAMS (Bouvier 1994, Bouvier & Forestini 1995, Keppens et al. 1995, Soderblom et al. 1993).

There might be other reasons, however, why we failed to measure a rotational period for P19, P94, and P146. For instance, the small $v \sin i$ of these stars may merely indicate that they are viewed nearly along their rotational axis (i.e., small $\sin i$). In such a geometry, the projected surface of a starspot remains nearly the same during the whole rotational cycle, thus inducing negligible amplitudes of photometric modulation. This might be the case for P19 whose light curve does not show variations significantly larger than the photometric errors. P94's and P146's light curves, however, exhibit variations with a maximum amplitude of about 0.1 mag. If due to starspots, the lack of a periodicity could arise from a spot lifetime being shorter than the rotational period. We are therefore unable to conclude on the true rotation rate of these 3 seemingly slow rotators.

For P12, however, we find a surprisingly short photometric period of 0.6d, which translates into an equatorial velocity of 93 km.s^{-1} , while $v \sin i$ is measured to be less than 10 km.s^{-1} . Even if we accept the alternative period of 1.47d, which appears as a mere alias of the 0.6d period, the true velocity would still be of 38 km.s^{-1} , implying an inclination angle of 15° at most for $R_* = 1.1 R_\odot$. In all cases then, P12 appears to be a fast rotator seen almost pole-on, which may also account for the fact that it is one of the stars with a detected period which exhibits a very low amplitude of modulation.

All the other stars for which we succeeded in measuring a period turn out to be moderate rotators, with periods in the range from 1.5 to 3.7d, corresponding to equatorial velocities between 14 and 36 km.s^{-1} . The $\sin i$ values computed from the rotational period and projected velocity are listed in Table 1: it shows that most stars with detected periods are seen at high inclination ($\sin i \geq 0.89$, with the exception of P12 above), which probably partly results from an observational bias since the contrast of the rotational modulation by spots increases for stars seen nearly equator-on.

We emphasize that the selection of the stellar sample was based only on the star's spectral type and their probable membership to the cluster. At the time of this selection, the $v \sin i$ were unknown and could therefore not be used as a selection

criterion. Therefore, as far as rotation is concerned, this sample can be considered as randomly selected. It is then interesting to note that we did not detect any period longer than 4d, though in principle we are able to measure periods up to 10d. This result suggests a relative deficiency of very slow rotators among the G-K dwarfs of IC 4665, with periods in the 4-10d range as observed for a number of late-type dwarfs in the Pleiades cluster (Prosser et al. 1995).

A similar conclusion was reached by Prosser & Giampapa (1994) from $v \sin i$ measurements, namely: only 3 over 15 G-K dwarfs in IC 4665 were found to have a $v \sin i$ less than 10 km.s^{-1} . This fractional number of slow rotators is close to that observed in the 50 Myr-old Alpha Per cluster ($\simeq 25\%$) but much smaller than that derived for the 70 Myr-old Pleiades cluster ($\simeq 50\%$). The increasing fraction of slow rotators in aging clusters results from the rapid braking of late-type dwarfs on the ZAMS. Therefore, the small fraction of slow rotators found in our randomly selected, but admittedly small, sample suggests that IC 4665 is closer in age to the Alpha Persei cluster than to the Pleiades.

Conversely, IC 4665 cannot be much younger than 40 Myr according to the location of its late-type members in the H-R diagram (Prosser & Giampapa 1994). An independent argument for the stars in IC 4665 being quite close to or even on the ZAMS, as opposed to being pre-main sequence stars, is provided by their small-amplitude photometric variability. The photometric amplitudes are found to be at most 0.1 mag and is often 0.05 mag or less among IC 4665's G-K dwarfs. Such a range of amplitudes is quite similar to that measured for late-type dwarfs, slow and rapid rotators alike, in the Alpha Persei and Pleiades clusters (e.g., Prosser et al. 1995). But it is significantly smaller than the amplitudes of modulation exhibited by pre-main sequence stars with an age of 10 Myr or less: in most weak-line T Tauri stars, the amplitude of rotational modulation ranges between 0.1 and 0.3 mag (Bouvier et al. 1993, 1995). The small-scale photometric variability of IC 4665 G-K dwarfs thus confirms that these stars are significantly older than T Tauri stars.

In spite of their different evolutionary status, IC 4665 dwarfs and weak-line T Tauri stars nevertheless have strikingly similar rotational periods (1-4day), a result which is not unexpected in the framework of current models of PMS angular momentum evolution (see Bouvier 1994 and references therein). That starspots are much smaller in young cluster dwarfs than in T Tauri stars, as indicated by their lower amplitudes of variability, cannot therefore be ascribed to different rotation rates. Instead, we believe that the declining starspot activity from the pre-main sequence to the ZAMS results from the retreat of the convective zone, thus leading to a reduced efficiency of the internal dynamo producing the surface magnetic field. Surprisingly enough, this decline of surface magnetic activity, indicated at the photospheric level by the size of starspots decreasing with age, is not seen at the coronal level, as weak-line T Tauri stars and moderate rotators in young clusters exhibit very similar level of X-ray fluxes (Stauffer et al. 1994).

5. Conclusion

The primary aim of this study was to search for very slow rotators among late-type dwarfs of the IC 4665 cluster. Although we were able to derive the equatorial velocity for half the stars in our sample, no slow rotators ($P \geq 4$ days) were found. The failure to detect long rotational periods is unlikely to be entirely the result of an observational bias but suggests instead a true deficiency of slow rotators in IC 4665. Such a paucity of very slow rotators needs to be confirmed by more sensitive techniques such as the Ca II H&K monitoring of young clusters dwarfs.

Among the 9 IC 4665 late-type stars with known rotational periods, 6 are moderate rotators with equatorial velocities in the range from 14 to 25 km.s^{-1} , and the remaining 3 are fast rotators ($V_{eq} \geq 36 \text{ km.s}^{-1}$). More rotational period measurements are clearly needed to improve the determination of the equatorial velocity distribution of these stars. Nevertheless, from the preliminary results reported here, it appears that the relative fraction of slow/moderate/fast rotators (0/6/3) is in good qualitative agreement with the predictions of recent models of angular momentum evolution of young solar-type stars.

Acknowledgements. We thank F.X. Nélva for assistance during the observations at OHP. Some of this research was performed at the Lowell Observatory 31-inch telescope which, under an agreement with Northern Arizona University and the NURO Consortium, is operated 60% of the time as the National Undergraduate Research Observatory. C.P. was supported under NASA Grant No. NAGW-2698.

Special thanks to D.H. Roberts et al. for their helpful and performing CLEAN algorithm.

References

- Allen C.W., 1976, *Astrophysical quantities* 3rd Ed. (London, Athlone)
- Bouvier J. 1991, in: *Angular Momentum Evolution of Young Stars*, ed. S. Catalano & J.R. Stauffer, p.41 (NATO ASI Series)
- Bouvier J. 1994, in: *The Eighth Cambridge Workshop on Cool Stars, Stellar System, and the Sun*, ed. J.-P. Caillault, ASP Conf. Ser., Vol.64, p.151
- Bouvier J., Forestini M. 1995, in: "Circumstellar Dust Disks and Planet Formation", 10th IAP meeting, ed. R. Ferlet, in press
- Bouvier J., Cabrit S., Fernandez M., Martin E.L., Matthews J.M 1993, *A&A* 272, 167
- Bouvier J., Covino E., Kovo O., Martin E.L., Matthews J.M., Terrane-gra L., Beck S.C. 1995, *A&A* in press
- Cameron A.C., Campbell C.G. 1993, *A&A* 274, 309
- Dworetzky M.M. 1983, *MNRAS* 203, 917
- Edwards S. et al. 1993, *AJ* 106, 372
- Hartmann L.W. 1991, in: *Angular Momentum Evolution of Young Stars*, ed. S. Catalano & J.R. Stauffer, p.379 (NATO ASI Series)
- Horne J.H., Baliunas S.L. 1986, *ApJ* 302, 757
- Keppens R., MacGregor K.B., Charbonneau P. 1995, *A&A* 294, 469
- King A.R., Regev O. 1994, *MNRAS* 268, L69
- Konigl A. 1991, *ApJ* 370, L39
- Mermilliod J.C. 1981, *A&AS* 44, 467
- O'Dell M.A., Collier Cameron A., 1993, *MNRAS* 262, 521
- Prosser C.F. 1991, thesis, Univ. of Calif. Santa Cruz.
- Prosser C.F. 1992, *AJ* 103, 488
- Prosser C.F. 1993, *AJ* 105, 1441

- Prosser C.F., et al. 1993, *PASP* 105, 1407
Prosser C.F., Giampapa M.S. 1994, *AJ* 108, 964
Prosser C.F. 1994, *AJ* 107, 1422
Prosser C.F. et al., 1995, *PASP* 107, 211
Roberts D.H., Lehar J., Dreher J.W. 1986, *AJ* 93, 968
Scargle J.D. 1982, *ApJ* 263, 835
Soderblom D.R., Stauffer J.R., MacGregor K.B., Jones B. 1993, *ApJ* 409, 624
Stauffer J.R., Hartmann L.W., Jones B.F., McNamara B.R. 1989, *ApJ* 342, 285
Stauffer J.R. 1991, in: *Angular Momentum Evolution of Young Stars*, ed. S. Catalano & J.R. Stauffer, p.117 (NATO ASI Series)
Stauffer J.R., Caillault J.-P., Gagné M., Prosser C.F., Hartmann L.W. 1994, *ApJS* 91, 625
Stetson P.B. 1987, *PASP* 99, 191
Shu F., Najita J., Ostriker E., Wilkin F., Ruden S., Lizano S. 1994, *ApJ* 429, 781
Van Leeuwen F., Alphenaar P. 1982, *ESO Messenger*, No. 28, 15
Van Leeuwen F., Alphenaar P., Meys J.J.M. 1987 *A&AS* 67, 483